

## Effects of an external magnetic field on shallow donor levels in semiconductors

Yao-Ming Mu, Jian-Ping Peng, Pu-Lin Liu, and Sue-Chu Shen  
*Chinese Center of Advanced Science and Technology (World Laboratory), P.O. Box 8730,  
Beijing 100080, People's Republic of China*  
and *National Laboratory for Infrared Physics, Shanghai Institute of Technical Physics,  
Academia Sinica, Shanghai 200083, People's Republic of China\**

Jing-Bing Zhu

*Institute of Semiconductors, Academia Sinica, P.O. Box 912, Beijing 100083, People's Republic of China*  
(Received 31 July 1992; revised manuscript received 24 March 1993)

An extension of Faulkner's method for the energy levels of the shallow donor in silicon and germanium at zero field is made in order to investigate the effects of a magnetic field upon the excited states. The effective-mass Hamiltonian matrix elements of an electron bound to a donor center and subjected to a magnetic field  $\mathbf{B}$ , which involves both the linear and quadratic terms of magnetic field, are expressed analytically and matrices are solved numerically. The photothermal ionization spectroscopy of phosphorus in ultrapure silicon for magnetic fields parallel to the  $[1,0,0]$  and  $[1,1,1]$  directions and up to 10 T is explained successfully.

### I. INTRODUCTION

Since the original theoretical works<sup>1,2</sup> on donor states in silicon and germanium in 1954–1955, the effective-mass theory (EMT) of impurity states in semiconductors is now sufficiently complete and accurate to explain in a satisfactory way the conventional infrared excitation spectra of shallow donors in silicon and germanium. Up to now, the Faulkner variational method<sup>3</sup> has been the most accurate method of calculation of donor energy levels in the absence of magnetic field. Shallow donor electronic states in semiconductors in the presence of the magnetic field along the  $z$  direction have been theoretically mostly studied by different variational calculations. For the case where the external magnetic field makes an angle with the  $z$  direction, it is customary to assume that only the  $z$  component of the magnetic field has an appreciable effect.<sup>4,5</sup> Using the perturbation method, Pajot<sup>6</sup> took into account the magnetic Hamiltonian, including some quadratic terms and perpendicular magnetic-field components. They obtained improved agreement for the energy splitting of donor transitions in silicon at high fields. However, they still neglected some terms in the Hamiltonian. In this paper, we deal with the full magnetic Hamiltonian by the Faulkner variational method. Faulkner's model allows us to evaluate analytically all terms in the Hamiltonian. Our results could be used where the EMT approximation is valid.

The Zeeman effects of donor impurities in semiconductors have been frequently studied using far-infrared (FIR)-absorption spectroscopy and have yielded important information about the electronic structure of donors. But these experiments were limited by linewidth, due in part to the relatively high doping concentration required by FIR absorption and high compensation broadening. Recent advances in semiconductor purification have made possible better measurements of Zeeman spectra of shal-

low impurities in semiconductors by photothermal ionization spectroscopy (PTIS). Navarro<sup>5</sup> measured the Zeeman spectra of shallow donors in ultrapure germanium with PTIS. In previous papers,<sup>7,8</sup> we reported the experimental results of a photothermal ionization spectroscopy measurement of Zeeman effects of phosphorus in ultrapure silicon. These experimental results are discussed and explained in this paper.

The organization of this paper is as follow. Section II briefly describes our experimental results. Our theoretical method is presented in Sec. III. In Sec. IV theoretical results are applied to investigate the energy levels of phosphorus in silicon. The magnetic-field dependence of the absorption intensity of some spectra is explained qualitatively by our theory. The change of spectroscopy intensity reflects directly the mixture of donor states in the magnetic field. The brief conclusion is presented in Sec. V.

### II. EXPERIMENT RESULTS

Our samples come from an ultrapure silicon single crystal with phosphorus as the main residual impurity, grown by the zone-melting technique. They are orientated by  $x$  rays, and the orientation error is less than  $\pm 0.5^\circ$ . The sample dimensions are  $3.5 \times 7 \times 8$  mm<sup>3</sup> and their resistivity is 450  $\Omega$  cm at room temperature. A technique which combines ion implantation and fast lamp annealing has been developed for preparing perfect Ohmic contacts for ultrapure silicon at helium temperature. The sample was mounted on the homemade sample holder and put into the stainless-steel Dewar with He as the exchange gas. The temperature was measured by a calibrated Oxford carbon thermometer. The magnetic field was provided by an Oxford superconductor magnetic system (S11/12L-40-13). The uncertainty of the magnetic field in the sample was estimated to be  $< 2\%$ . The photothermal

ionization spectra were recorded by means of a rapid-scan Fourier-transform spectrometer, Bruker FTS-113v. The experiment has been described in detail in Refs. 7 and 8. The spectrometer and magnetic system have been calibrated very accurately. The experimental error arising from inaccuracies in locating the position of the photoconductivity peaks is less than  $0.3 \text{ cm}^{-1}$ . We estimate that experimental errors arising from these inaccuracies are less than  $1 \text{ cm}^{-1}$ . The typical experimental spectra are shown in Fig. 1, where the spectra at different magnetic-field strengths and different sample orientations are demonstrated as curves *a*, *b*, and *c* for transitions from the  $1s$  ground state to excited states of the phosphorus shallow donor in silicon. Figure 2 presents the Zeeman diagram that summarizes the resultant magnetic-field dependence of the observed  $P$ -like transitions of the phosphorus donor for magnetic field parallel to the  $[1,0,0]$  direction. The full lines are drawn for visual aid. The lines related with the states in different valley are labeled with the subscripts *A* or *B*.

### III. THEORY

In the effective-mass approximation, the Hamiltonian of an electron bound to a donor center and subjected to a magnetic field  $\mathbf{B}$  defined by a vector potential  $\mathbf{A}=(\mathbf{B}\times\mathbf{r})/2$  can be written as

$$H=(\mathbf{P}-e\mathbf{A}/c)^2/2m^*-\frac{e^2}{\kappa r} \quad (1)$$

$$=H_0+H_1+H_2, \quad (2)$$

where  $H_0$  is the effective-mass Hamiltonian of the donor electron at zero field, and reads using  $a=\hbar^2\kappa/m_\perp e^2$  as a length unit, and  $R=m_\perp e^4/2\hbar^2\kappa^2$  as an energy unit:

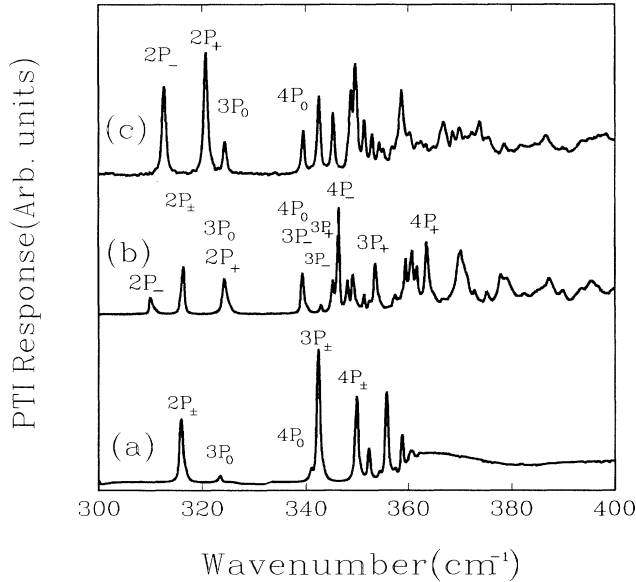


FIG. 1. PTI spectra of phosphorus donors in ultrapure silicon in the wave-number region from  $300$  to  $400 \text{ cm}^{-1}$  for (a)  $B=0$ , (b)  $B=3 \text{ T}$  and  $B\parallel[1,0,0]$ , and (c)  $B=3 \text{ T}$  and  $B\parallel[1,1,1]$  at temperature  $T=20 \text{ K}$  and spectral resolution  $0.15 \text{ cm}^{-1}$ .

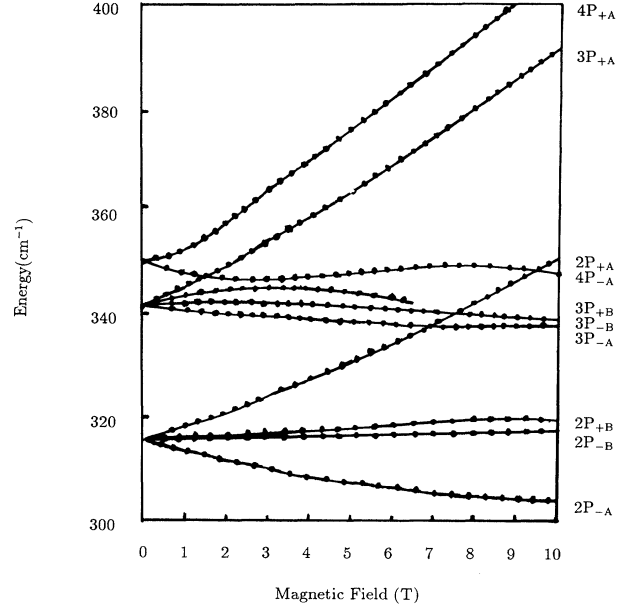


FIG. 2. The Zeeman diagram of the phosphorus donor transitions from the  $1s$  ground state to  $P$ -like excited states in the wave-number region from  $300$  to  $400 \text{ cm}^{-1}$  for the magnetic field along the  $[1,0,0]$  direction.

$$H_0=-\nabla^2+(1-\gamma)\frac{\partial^2}{\partial z^2}-\frac{2}{r}, \quad (3)$$

with  $\gamma=m_\perp/m_\parallel$ . The eigenproblem of  $H_0$  has been solved by Faulkner<sup>3</sup> via the Raleigh-Ritz approach. The  $N$  orthonormal functions  $\varphi_{nlm}$  are used to set up the Hermitian matrix

$$\varphi_{nlm}=\left[\frac{\beta}{\gamma}\right]^{1/4}\psi_{nlm}\left[x,y,\left[\frac{\beta}{\gamma}\right]^{1/2}z\right], \quad (4)$$

where  $\psi_{nlm}(x,y,z)$  represents the normalized hydrogenic wave functions,  $\psi_{nlm}(x,y,z)=R_{nl}(\alpha_{lm},r)Y_{lm}(\theta,\varphi)$ , and

$$R_{nl}(\alpha_{lm},r)=\frac{2\alpha_{lm}^{3/2}}{n^2}\left[\frac{(n-l-1)!}{[(n+l)!]^3}\right]^{1/2}\left[\frac{2\alpha_{lm}r}{n}\right]^l \times \exp\left[-\frac{\alpha_{lm}r}{n}\right]L_{n-l-1}^{2l+1}\left[\frac{2\alpha_{lm}r}{n}\right].$$

$\alpha_{lm}$  and  $\beta$  are adjustable parameters. The Hamiltonian matrix element  $\langle n'l'm'|H_0|nlm\rangle$  can be expressed analytically.

The linear and quadratic magnetic-field terms  $H_1$  and  $H_2$  can be written with coordinate transformation  $z=\eta_{pm}z$ ,  $\eta_{pm}=(\gamma/\beta)^{1/2}$ ,

$$H_1=\gamma^*\left[\eta_{pm}L_xB_x+\eta_{pm}L_yB_y+L_zB_z +i\eta_{pm}(1-\beta)(yB_x-xB_y)\frac{\partial}{\partial z}\right], \quad (5)$$

where  $\gamma^*=\hbar eB/2Rm_\perp C$ . The last term in  $H_1$  has been

neglected in previous calculations for Si:

$$H_2 = \left[ \frac{\gamma^*}{2} \right]^2 [\eta_{pm}^2 z^2 (B_x^2 + B_y^2) - 2\eta_{pm} B_z (xB_x + yB_y) + (x^2 + y^2)B_z^2 + \gamma(yB_x - xB_y)^2]. \quad (6)$$

$H_1$  and  $H_2$  can be written in the spherical coordinate as

$$H_1 = H_{1a} + H_{1b}, \quad (7)$$

$$H_{1a} = \gamma^* B [\eta_{pm} (L_x \sin\varphi_B + L_y \cos\varphi_B) \sin\theta_B + L_z \cos\theta_B], \quad (8)$$

$$H_{1b} = -i\gamma^* B \eta_{pm} (\beta - 1) \sin\theta \sin\theta_B \times (\cos\varphi \sin\varphi_B - \sin\varphi \cos\varphi_B) \times \left[ r \cos\theta \frac{\partial}{\partial r} - \sin\theta \frac{\partial}{\partial \theta} \right], \quad (9)$$

$$H_2 = H_{2a} + H_{2b} + H_{2c}, \quad (10)$$

$$H_{2a} = \left[ \frac{\gamma^* B r}{2} \right]^2 [\cos^2\theta_B \sin^2\theta + \eta_{pm}^2 \cos^2\theta \sin^2\theta_B + \gamma \sin^2\theta_B \sin^2\theta (\sin^2\varphi_B \cos^2\varphi + \cos^2\varphi_B \sin^2\varphi)], \quad (11)$$

$$H_{2b} = -2\eta_{pm} \left[ \frac{\gamma^* B r}{2} \right]^2 \cos\theta \sin\theta \cos\theta_B \sin\theta_B \times (\sin\varphi \sin\varphi_B + \cos\varphi \cos\varphi_B), \quad (12)$$

$$H_{2c} = -2\gamma \left[ \frac{\gamma^* B r}{2} \right]^2 \sin^2\theta_B \sin^2\theta \sin\varphi_B \times \cos\varphi_B \sin\varphi \cos\varphi, \quad (13)$$

where  $(r, \theta, \varphi)$  is the position of the electron and  $(B, \theta_B, \varphi_B)$  is the spherical coordinate of the magnetic field  $\mathbf{B}$ . We take the  $[1, 0, 0]$  axis as the  $z$  direction.

The  $H_{1a}$  term will mix states of different  $m$ 's but the same  $(n, l)$  when  $\mathbf{B}$  is not parallel to the  $z$  axis. The  $H_{1b}$  term is zero when  $\mathbf{B}$  is parallel to the  $z$  axis. It can mix states of different values of  $m$ . When  $\mathbf{B}$  lies in a  $(011)$  or  $(01\bar{1})$  plane,  $H_{2a}$  is invariant under the inversion and rotation about the  $z$  axis, and it cannot cause the interaction of levels of different parity or projection of the angular momentum.  $H_{2b}$  is equal to zero when  $\mathbf{B}$  is parallel to the  $z$  axis or lies in  $xy$  plane.  $H_{2c}$  vanishes when  $\mathbf{B}$  is parallel to the  $z$  axis.  $H_{2b}$  and  $H_{2c}$  are not invariant under rotation about the  $z$  axis, so that the states of different values of  $m$  can be mixed by them. All terms in the Hamiltonian cannot mix states of different parities.

Straightforward but tedious operations with the properties of the  $R_{nl}(r)$  and  $Y_{lm}(\theta, \varphi)$  yield analytical expressions of the Hamiltonian matrix elements

$\langle n'l'm'|H_1|nlm\rangle$  and  $\langle n'l'm'|H_2|nlm\rangle$ . They are given in the Appendix. These formulas can be used to set up a Hamiltonian matrix of any desired order to investigate the shallow donor levels in semiconductors for which the EMT is valid.

#### IV. NUMERICAL RESULTS FOR PHOSPHORUS IN SILICON

We choose the valleys (ellipsoids) 1, 2, 3, 4, 5, and 6 in silicon to lie along the  $z, \bar{z}, x, \bar{x}, y,$  and  $\bar{y}$  axes, respectively, and the correction among valleys is neglected for the magnetic field along the  $[1, 1, 1]$  direction, i.e., the one-valley approximation. For the magnetic field along  $[1, 0, 0]$ , because only two of the six valleys have their axis of symmetry along the field and the other four have their symmetry axes perpendicular to the field, the energy of the ground state is obtained by finding the one-valley energy for each of the orientations and their weighted average (weighting them by either  $\frac{2}{6}$  or  $\frac{4}{6}$ ).<sup>9</sup> The following parameters have been used for numerical calculations of phosphorus in silicon:

$$\gamma = 0.2079, \quad R = 19.93 \text{ meV}, \quad m_{\perp} = 0.1905 m_0.$$

We consider up to the principal quantum number  $n = 5$ , i.e., 29 hydrogenic wave functions for the even-parity states. For the odd-parity states, we deal with  $n = 2-6$ , i.e., 47 hydrogenic wave functions. The  $29 \times 29$  and  $47 \times 47$  Hamiltonian matrixes are solved numerically. We assume that  $\eta_{pm}$  is independent of  $m$ , i.e., at a given magnetic field all states of a given parity are assigned the same value of  $\eta_p$  for simplicity. Other parameters are  $\alpha_{l,m}$  in the wave functions  $R_{nl}(\alpha_{l,m}, r)$  and we assume that  $\alpha_{l,m}$  depends on the  $|m|$ , i.e.,  $\alpha_{l,m} = \alpha_{l,|m|}$ . Therefore, there are 13 variational parameters for these odd-parity states, and 10 for these even-parity states. All variational parameters are determined by an optimization search which minimizes the sum of the energy eigenvalues for different magnetic-field strengths. Our parameters are functions of magnetic field  $B$ , and we consider field-dependent wave functions.

It is well known that the effective-mass approximation fails to predict correctly the ground-state energy of shallow donor. The central-cell correction, i.e., the non-Coulomb nature of the potential in the immediate vicinity of an impurity, must be considered.<sup>4,9-11</sup> We add phenomenologically a parameter term  $\Delta$  to the diagonal matrix element  $\langle 1S|H|1S\rangle$  and assume that the parameter  $\Delta$  is independent of magnetic field. This is determined by fitting the energy of the  $2P_0$  state at zero magnetic field. We obtain  $\Delta \approx -115 \text{ cm}^{-1}$ .

It is not easy to choose the  $P$ -like energy levels among the 47 eigenvalues of odd-parity states due to the strong mixture of electronic states at high magnetic field. We utilize the experimental results and treat the eigenvalues which are closest to the measurement as theoretical results.

In order to estimate errors arising from the fact that a basis set of finite size is employed, we have investigated how sensitive energies are to basis size. The larger the principal quantum number, the more sensitive the energy

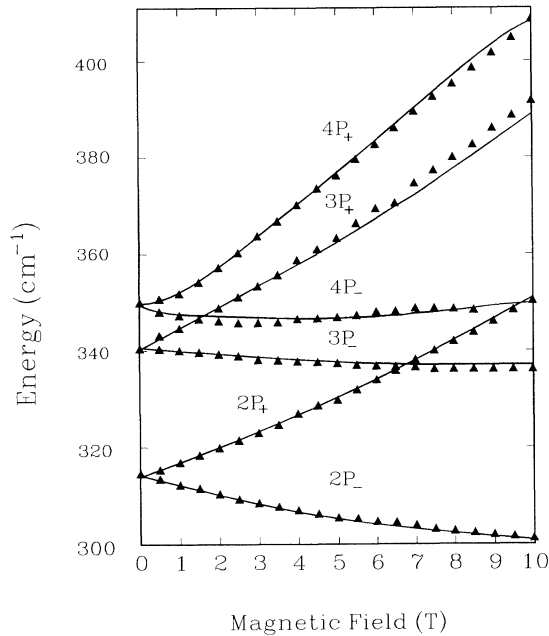


FIG. 3. The comparison of the calculated magnetic-field dependence of transitions from the  $1s$  ground state to  $2P_{\pm}$ ,  $3P_{\pm}$ , and  $4P_{\pm}$  excited states under magnetic field along  $[1,0,0]$ , with experimental observation.

of the state is to basis size. For example, if we consider up to the principal quantum number  $n=4$  for even-parity states, the energy change of the state with  $n=4$  (the  $4S$  state) is about 3% and much larger than that of  $1S$  state. Because we are interested only in the  $1S$  ground state, it seems that the number of basis functions for the even-parity state can be reduced, but  $n$  cannot be less than 3. If we consider up to principal quantum number  $n=5$  for odd-parity states, the energy change of  $4P_0$  is about  $2 \text{ cm}^{-1}$ , and that of  $4P_{\pm}$  is about  $2.5 \text{ cm}^{-1}$  at  $B=0 \text{ T}$ , and they are about 2 and  $3 \text{ cm}^{-1}$  at  $B=10 \text{ T}$ , respectively. If we increase  $n$ , energy changes in  $4P_0$  and  $4P_{\pm}$  are less than  $1 \text{ cm}^{-1}$ . We can obtain more accurate results by considering additional basis functions, but the number of parameters increases very quickly.

We compute the  $P$ -like energy levels of phosphorus in silicon as a function of the magnetic field along the  $[1,0,0]$  and  $[1,1,1]$  directions and up to 10 T. A comparison between the observed and calculated values is shown in Figs. 3 and 4. Theoretical results are in good agreement with experimental observation. Furthermore, we obtain a better agreement with experiment than previous calculations, because the full magnetic Hamiltonian and field-dependent hydrogenic wave functions are treated. The discrepancies between theory and experiment approach the experimental error. From Figs. 3 and 4, it can be seen that the crossing of the  $2P_{+}$  line with the  $3P_{-}$  for the magnetic field along  $[1,0,0]$ , and the prevented crossing of the  $2P_{+}$  line with the  $3P_0$  for the magnetic field along  $[1,1,1]$ , which have been observed in many experi-

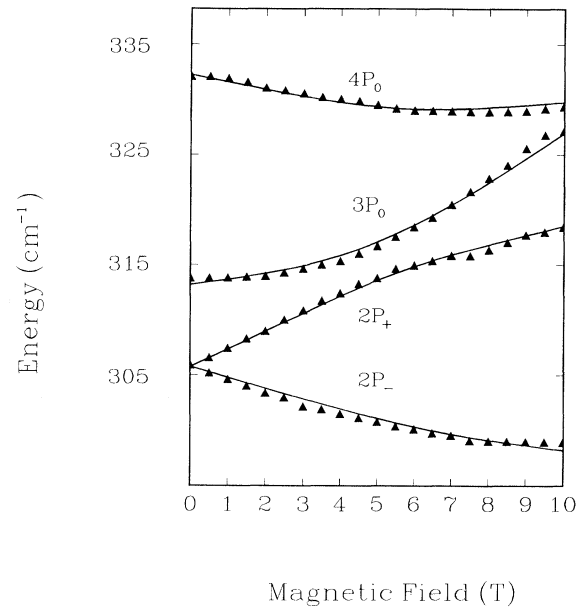


FIG. 4. The comparison of the calculated magnetic-field dependence of transitions from the  $1s$  ground state to  $2P_{\pm}$ ,  $3P_0$ , and  $4P_0$  excited states under magnetic field along  $[1,1,1]$ , with experimental observation.

ments,<sup>12,13</sup> are explained satisfactorily. Pajot's perturbation method<sup>6</sup> applied zero-field hydrogenic wave functions and obtained a qualitative agreement with experimental results, but the agreement is not quantitatively so good.

## V. CONCLUSION

We extend Faulkner's method and obtain analytical expressions of full magnetic Hamiltonian matrix elements for an electron bound to a donor center and subjected to an external magnetic field. The improved agreement between calculated and measured results is achieved using field-dependent hydrogenic waves. Results show that the magnetic-field dependence of transitions from ground states to  $P$ -like excited states of phosphorus in silicon can be explained reasonably by the EMT approximation with field-dependent hydrogenic waves and full magnetic Hamiltonian terms. Our formulas can be applied to cases where the EMT approximation is valid.

## ACKNOWLEDGMENT

This work was supported by the Chinese Science Foundation.

## APPENDIX

In this appendix, the Hamiltonian matrix elements for  $H_1$  and  $H_2$  are evaluated analytically, using the properties of the  $R_{nl}$  and  $Y_{lm}$ .

Let us define the following functions:

$$\begin{aligned}
J^K(n, l, \alpha_{lm}; n', l', \alpha_{l'm'}) &= \int_0^\infty r^K R_{nl}(\alpha_{lm} r) R_{l'm'}(\alpha_{l'm'} r) dr \\
&= 2^{l+l'+2} [(n+l)!(n-l-1)!(n'+l')!(n'-l'-1)!]^{1/2} n^{-2} \alpha_{lm} \left( \frac{\alpha_{lm}}{\alpha_{l'm'}} \right)^{1/2} \\
&\quad \times \sum_{\substack{s'=0 \\ s=0}}^{n'-l'-1} \frac{(-2)^{s+s'} \left[ 1 + \frac{n'\alpha_{lm}}{n\alpha_{l'm'}} \right]^{-(l+l'+s+s'+k+1)} \left( \frac{n'\alpha_{lm}}{n\alpha_{l'm'}} \right)^{l+s} (l+l'+s+s'+k)!}{(n-l-s-1)!(2l+s+1)!s!(n'-l'-s'-1)!(2l'+s'+1)!s'!},
\end{aligned}$$

$$\begin{aligned}
D^K(n, l, \alpha_{lm}; n', l', \alpha_{l'm'}) &= \int_0^\infty r^K R_{nl}(\alpha_{lm} r) \frac{\partial R_{l'm'}(\alpha_{l'm'} r)}{\partial r} dr \\
&= l' J^{K-1}(n, l, \alpha_{lm}, n', l', \alpha_{l'm'}) - \frac{\alpha_{l'm'}}{n'} J^K(n, l, \alpha_{lm}, n', l', \alpha_{l'm'}) \\
&\quad - \frac{2\alpha_{l'm'}}{n'} J_D^K(n, l, \alpha_{lm}, n', l', \alpha_{l'm'}) \theta(n'-l'-2),
\end{aligned}$$

where

$$\begin{aligned}
J_D^K(n, l, \alpha_{lm}; n', l', \alpha_{l'm'}) &= 2^{l+l'+2} [(n+l)!(n-l-1)!(n'+l')!(n'-l'-1)!]^{1/2} n^{-2} \alpha_{lm} \left( \frac{\alpha_{lm}}{\alpha_{l'm'}} \right)^{1/2} \\
&\quad \times \sum_{\substack{s'=0 \\ s=0}}^{n'-l'-1} \frac{(-2)^{s+s'} \left[ 1 + \frac{n'\alpha_{lm}}{n\alpha_{l'm'}} \right]^{-(l+l'+s+s'+k+1)} \left( \frac{n'\alpha_{lm}}{n\alpha_{l'm'}} \right)^{l+s} (l+l'+s+s'+k)!}{(n-l-s-1)!(2l+s+1)!s!(n'-l'-s'-2)!(2l'+s'+2)!s'!}
\end{aligned}$$

and

$$\theta(x) = \begin{cases} 1, & x \geq 0 \\ 0, & x < 0. \end{cases}$$

The Hamiltonian matrix elements  $\langle n, l, m | H_{1a} | n', l', m' \rangle$  can be evaluated conveniently. The analytic expression of  $\langle n, l, m | H_{2a} | n', l', m' \rangle$  for  $\mathbf{B}$  lying in a  $(0, 1, 1)$  or  $(0, 1, \bar{1})$  plane has been given by Pajot.<sup>6</sup> In what follows, we give the other matrix elements:

$$\langle n, l, m | H_{2b} | n', l, m \pm 1 \rangle = \pm C_{H_{2b}}(n, l, m; n', l, m \pm 1) \frac{\sqrt{(l \mp m)(l \pm m + 1)}}{2(2l + 1)} \left[ \frac{l \mp m - 1}{2l - 1} - \frac{l \pm m + 2}{2l + 3} \right],$$

$$\begin{aligned}
\langle n, l, m | H_{2b} | n', l + 2, m \pm 1 \rangle &= \mp C_{H_{2b}}(n, l, m; n', l + 2, m \pm 1) \\
&\quad \times \frac{1}{2(2l + 3)} \left[ \frac{(l \mp m + 1)(l \pm m + 3)(l \pm m + 2)(l \pm m + 1)}{(2l + 5)(2l + 1)} \right]^{1/2},
\end{aligned}$$

$$\langle n, l, m | H_{2b} | n', l - 2, m \pm 1 \rangle = \pm C_{H_{2b}}(n, l, m; n', l - 2, m \pm 1) \frac{1}{2(2l - 1)} \left[ \frac{(l \mp m)(l \mp m - 1)(l \mp m - 2)(l \pm m)}{(2l + 1)(2l - 3)} \right]^{1/2},$$

where

$$C_{H_{2b}}(n, l, m, n', l', m \pm 1) = -2\eta_{pm} \left[ \frac{\gamma^* \mathbf{B}}{2} \right]^2 (\cos\varphi_B \pm i \sin\varphi_B) \sin\theta_B \cos\theta_B J^4(n, l, \alpha_{lm}, n', l', \alpha_{l'm \pm 1}),$$

$$\langle n, l, m | H_{2c} | n', l, m \pm 2 \rangle = -C_{H_{2c}}(n, l, m, n', l, m \pm 2) \frac{\sqrt{(l \mp m - 1)(l \mp m)(l \pm m + 1)(l \pm m + 2)}}{2(2l + 1)} \left[ \frac{1}{2l - 1} + \frac{1}{2l + 3} \right],$$

$$\begin{aligned}
\langle n, l, m | H_{2c} | n', l + 2, m \pm 2 \rangle &= C_{H_{2c}}(n, l, m, n', l + 2, m \pm 2) \\
&\quad \times \frac{1}{2(2l + 3)} \left[ \frac{(l \pm m + 4)(l \pm m + 3)(l \pm m + 2)(l \pm m + 1)}{(2l + 1)(2l + 5)} \right]^{1/2},
\end{aligned}$$

$$\langle n, l, m | H_{2c} | n', l - 2, m \pm 2 \rangle = C_{H_{2c}}(n, l, m, n', l - 2, m \pm 2) \frac{1}{2(2l - 1)} \left[ \frac{(l \mp m)(l \mp m - 1)(l \mp m - 2)(l \mp m)}{(2l + 1)(2l - 3)} \right]^{1/2},$$

where

$$C_{H_{2c}}(n, l, m, n', l', m \pm 2) = \mp \gamma \left[ \frac{\gamma^* B}{2} \right]^2 \sin^2 \theta_B \sin \varphi_B \cos \varphi_B J^4(n, l, \alpha_{lm}; n', l', \alpha_{l'm \pm 2}),$$

$$\langle n, l, m | H_{1b} | n', l, m \pm 1 \rangle = \mp C_{H_{1b}}(m \pm 1) \frac{\sqrt{(l \mp m)(l \pm m + 1)}}{2(2l + 1)} \\ \times \left\{ \left[ \frac{(l + 1)(l \mp m - 1)}{2l - 1} + \frac{l(l \pm m + 2)}{2l + 3} \right] J^2(n, l, \alpha_{lm}; n', l, \alpha_{lm \pm 1}) \right. \\ \left. - \left[ \frac{l \mp m - 1}{2l - 1} - \frac{l \pm m + 2}{2l + 3} \right] D^3(n, l, \alpha_{lm}; n', l, \alpha_{lm \pm 1}) \right\},$$

$$\langle n, l, m | H_{1b} | n', l + 2, m \pm 1 \rangle = \mp \frac{C_{H_{1b}}(m \pm 1)}{2(2l + 3)} \left[ \frac{(l \mp m + 1)(l \pm m + 3)(l \pm m + 2)(l \pm m + 1)}{(2l + 5)(2l + 1)} \right]^{1/2} \\ \times [(l + 3)J^2(n, l, \alpha_{lm}; n', l + 2, \alpha_{l+2m \pm 1}) + D^3(n, l, \alpha_{lm}; n', l + 2, \alpha_{l+2m \pm 1})],$$

$$\langle n, l, m | H_{1b} | n', l - 2, m \pm 1 \rangle = \mp \frac{C_{H_{1b}}(m \pm 1)}{2(2l - 1)} \left[ \frac{(l \mp m)(l \mp m - 1)(l \mp m - 2)(l \pm m)}{(2l + 1)(2l - 3)} \right]^{1/2} \\ \times [(l - 2)J^2(n, l, m; n', l - 2, m \pm 1) - D^3(n, l, m; n', l - 2, m \pm 1)],$$

where

$$C_{H_{1b}}(m \pm 1) = (1 - \beta) \eta_{pm} \gamma^* B \sin^2 \theta_B (\pm \cos \varphi_B + i \sin \varphi_B).$$

\*Mailing address.

<sup>1</sup>C. Kittel and A. H. Mitchell, Phys. Rev. **96**, 1488 (1954).

<sup>2</sup>W. Kohn and J. M. Luttinger, Phys. Rev. **98**, 915 (1955).

<sup>3</sup>R. A. Faulker, Phys. Rev. **184**, 713 (1969).

<sup>4</sup>Y. Nisida and K. Horii, J. Phys. Soc. Jpn. **31**, 776 (1971).

<sup>5</sup>H. Navarro, J. Griffin, and E. E. Haller, J. Phys. C **21**, 1511 (1988).

<sup>6</sup>B. Pajot, F. Merlet, G. Taravella and Ph. Arcas, Can. J. Phys. **50**, 1106 (1972).

<sup>7</sup>J. B. Zhu, P. L. Liu, G. L. Shi, W. J. Liu, X. F. Lu, and S. C. Shen, Proc. SPIE **1575**, 584 (1991); S. C. Shen, *ibid.* **1575**, 161 (1991).

<sup>8</sup>J. B. Zhu, P. L. Liu, G. L. Shi, W. J. Liu, and X. C. Shen, Chin. J. Semicond. **13**, 232 (1992).

<sup>9</sup>C. Jagganath, E. R. Youngdale, D. M. Larsen, R. L. Aggarwal, and P. A. Wolff, Solid State Commun. **43**, 267 (1982).

<sup>10</sup>N. Lee, D. M. Larsen, and B. Lax, J. Phys. Chem. Solids **34**, 1817 (1973).

<sup>11</sup>N. Lee, D. M. Larsen, and B. Lax, J. Phys. Chem. Solids **35**, 401 (1973).

<sup>12</sup>S. Zwerdling, K. J. Button, and B. Lax, Phys. Rev. **118**, 975 (1960).

<sup>13</sup>B. Pajot, F. Merlet, and G. Taravella, Can. J. Phys. **50**, 2186 (1972).